Journal of Alloys and Compounds 509 (2011) 9460–9465

Contents lists available at ScienceDirect

Journal of Alloys and Compounds

journal homepage: www.elsevier.com/locate/jallcom

Magnetocaloric effect in composite structures based on ferromagnetic–ferroelectric $Pr_{0.6}Sr_{0.4}MnO_3/BaTiO_3$ perovskites

M. Triki [a,*], R. Dhahri [a], M. Bekri [b], E. Dhahri [a], M.A. Valente [c]

[a] Laboratoire de Physique Appliquée, Faculté des Sciences de Sfax, B. P. 1171, 3000 Sfax, Tunisia
[b] Physics Department, Rabigh College of Science and Art, King Abdulaziz University, P.O. Box 344, Rabigh 21911, Saudi Arabia
[c] Physics Department (I3N), Aveiro University, Campus Universitá rio de Santiago, 3800-193 Aveiro, Portugal

ARTICLE INFO

Article history:
Received 6 April 2011
Received in revised form 8 July 2011
Accepted 11 July 2011
Available online 23 July 2011

Keywords:
Ferromagnetic
Ferroelectric
Magnetic entropy
Landau expansion

ABSTRACT

We have prepared composite materials composed of ferromagnetic and ferroelectric compounds having the general formula $(1-x)(Pr_{0.6}Sr_{0.4}MnO_3)/x(BaTiO_3)$, with x is the molar ratio ($x = 0.0$, 0.03, 0.05, 0.10 and 0.30) using conventional ceramic double sintering process. We report the structural, magnetic and magnetocaloric properties of all samples. The presence of the two phases of $Pr_{0.6}Sr_{0.4}MnO_3$ (PSMO) and $BaTiO_3$ (BTO) was confirmed by X-ray diffraction (XRD) technique and the structural analysis. Magnetic measurements of magnetization versus temperature and magnetic applied field were performed. The temperature dependence of magnetization reveals that the composite samples show paramagnetic to ferromagnetic phase transition (PM–FM) when the temperature decreases. These samples have the same Curie temperature as the parent PSMO compound ($T_c \approx 273$ K). The magnetic entropy change $|\Delta S_M|$ was deduced from the $M(H)$ data by the Maxwell relation. Close to T_c, a large change in magnetic entropy has been observed in all samples. The maximum value of the magnetic entropy $|\Delta S_M^{max}|$ decreases from 2.88 J kg^{-1} K^{-1} for $x = 0$–1.86 J kg^{-1} K^{-1} for $x = 0.3$ for an applied magnetic field of 2 T. At this value of magnetic field the relative cooling power (RCP) decreases equally from 63 J kg^{-1} for the parent sample to 38.3 J kg^{-1} for $x = 0.3$. The temperature dependence of the Landau coefficients has been deduced using the Landau expansion of the magnetic free energy, indicating the second order nature of the magnetic transition.

1. Introduction

The mixed valence manganites with the general formula $Ln_{1-x}A_xMnO_3$ (Ln is a trivalent rare earth element and A is a divalent alkali-earth one) have renewed extensive interests thanks to their colossal magnetoresistance (CMR) effect and also to their potential applications in magnetoresistive transducers, magnetic sensors and magnetic refrigeration [1–4]. A big interest is being paid to multiferroic materials with coupled electric and magnetic properties because they can exhibit both electrical polarization induced by a magnetic field and magnetization induced by an electric field [5–9]. If these materials are to be used in practical applications, it is necessary to make a composite of magnetic and electric compounds with an improved magnetoelectric effect. Various such composites have been studied mainly showing enhancement of the CMR phenomena mostly observed near T_c and caused by the double exchange (DE) mechanism proposed by Zener in 1951 [10].

The extrinsic CMR is related to natural and artificial grain boundaries. Spin polarized tunneling or spin dependent scattering of the charge carriers at the grain boundaries seems to be responsible for this kind of CMR effects [11]. This extrinsic effect may enhance MR in a wide temperature range and can be more useful to satisfy practical applications in magnetic and switching of recording devices. Previous studies on magnetoelectric composites were focused on bulk samples composed of LCMO/BTO [12–14], LSMO/BTO [15,16], PCMO/BST [17,18] LCMO/PZT [19], etc. showing enhancement in MR and magnetoelectric couplings.

The aim of this article is to study the effect of the coexistence of both the ferroelectric $BaTiO_3$ with the ferromagnetic $Pr_{0.6}Sr_{0.4}MnO_3$ in many proportions on the structural, magnetic and magnetocaloric properties of these composites. In this paper we present especially the influence of the ferroelectric phase on the magnetic properties of ferromagnetic PSMO phase.

2. Experimental

The samples were prepared in three steps. At first, the PSMO phase was prepared through normal solid-state reaction route taking Pr_6O_{11}, $SrCO_3$ and MnO_2 in stoichiometric proportions. The mixed powders were presintered at 1000 °C for 24 h. The resulting powder was pressed into pellets, and then sintered at 1350 °C

* Corresponding author. Tel.: +216 21 501 866.
E-mail address: mtriki_fss@yahoo.fr (M. Triki).

0925-8388/$ – see front matter © 2011 Elsevier B.V. All rights reserved.
doi:10.1016/j.jallcom.2011.07.031

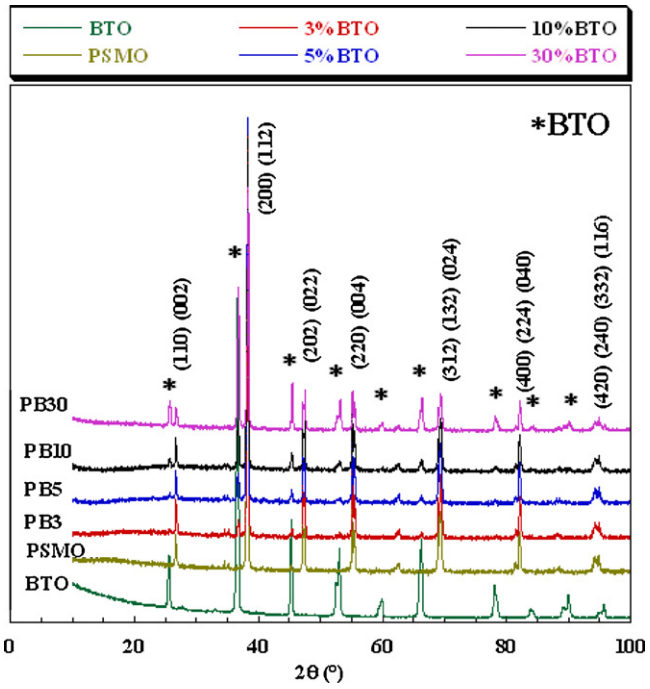

Fig. 1. XRD patterns of PSMO/BTO composites with varying compositions (asterisks are noted for BTO phase and *h k l* for PSMO phase).

for 24 h with intermediate regrinding and re-pelletizing. These pellets were rapidly quenched to room temperature in air in order to freeze the structure at the annealed temperature. Secondly, the ferroelectric phase, BTO was prepared by the same method as PSMO using $BaCO_3$ and TiO_2 in molar ratios as starting materials. BTO phase was presintered at 850 °C for 24 h and then pressed into pellets and sintered at 1000 °C for 24 h with intermediate regrinding and re-pelletizing. Finally, the composites were prepared by thoroughly mixing 3, 5, 10 and 30% of ferroelectric phase (BTO) with 97, 95, 90 and 70% of ferromagnetic phase (PSMO) respectively, and then were pelletized and sintered at 900 °C for 24 h. The obtained samples will be referred as, PB3, PB5, PB10 and PB30 respectively and PSMO for the parent compound ($x = 0$). The samples were characterized by X-ray powder diffraction at room temperature using Mo radiation and the structure refinement was carried out by the Rietveld analysis of the X-ray powder diffraction data. Magnetization measurements were carried out using a Foner magnetometer equipped with a super-conducting coil in different magnetic fields.

3. Results and discussion

3.1. X-ray diffraction analysis

Fig. 1 shows the powder X-ray diffraction patterns at room temperature for the parent PSMO and BTO samples and equally all synthesized composites. Rietveld refinement was performed for all the samples, we show in Fig. 2 the refinement for PB3 sample as an example. The analysis shows that the parent compounds are single phase with orthorhombic Pbnm space group for PSMO for which the lattice parameters are estimated as $a = 0.5481$ nm, $b = 0.5441$ nm and $c = 0.7673$ nm, and tetragonal P4mm space group for BTO with the lattice parameters $a = b = 0.3994$ nm and $c = 0.4027$ nm. As we can see in the composites, with the increase of BTO content, the peak intensity corresponding to BTO phase increases and also the peaks positions related to PSMO have no shift due to the addition of BTO, which indicates that the PSMO and BTO phases exist independently and form a solid mixture without any chemical reaction between the parent compounds during the heat treatment. For these samples, the estimated lattice parameters of the PSMO and BTO phases remained almost unchanged.

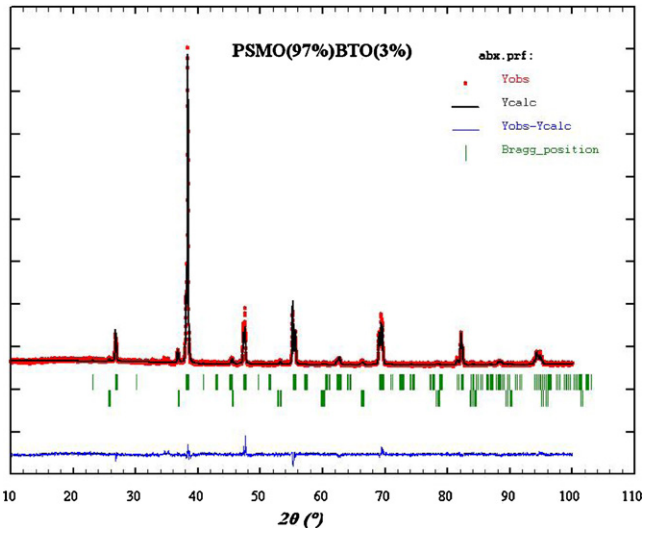

Fig. 2. XRD patterns of 0.97PSMO/0.03BTO composite. Squares indicate the experimental data and the calculated data is the continuous line overlapping them. The lowest curve shows the difference between experimental and calculated patterns. The vertical bars indicate the expected reflection positions.

3.2. Magnetic properties

Fig. 3 shows the temperature dependence of magnetization (M) measured at an applied magnetic field of 0.05 T. All composites show a paramagnetic–ferromagnetic transition when the temperature decreases. These composites have the same Curie temperature as the parent compound PSMO ($T_c \approx 273$ K) obtained from the peak in dM/dT versus temperature (T) plot and also by the temperature dependence of the inverse of magnetic susceptibility plot shown inset of Fig. 3 for the PSMO compound. The Curie temperature is not affected by the increase of BTO content. This is due to the fact that the PM–FM phase transition is an intrinsic and intragrain property. The observed constancy of T_c also indicates that stoichiometry of PSMO phase within the grains remains essentially unchanged as BTO is not accommodated within the perovskite structure and its

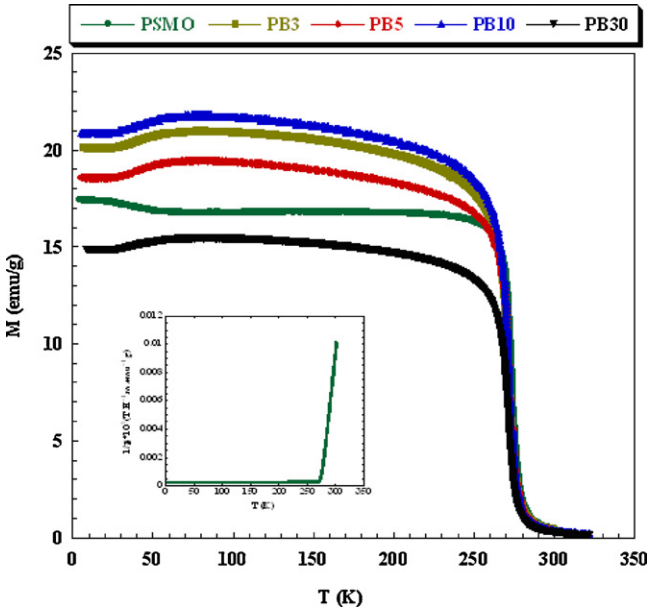

Fig. 3. Temperature dependence of magnetization for PSMO/BTO composites. The inset presents the temperature dependence of the inverse of the magnetic susceptibility for PSMO compound.

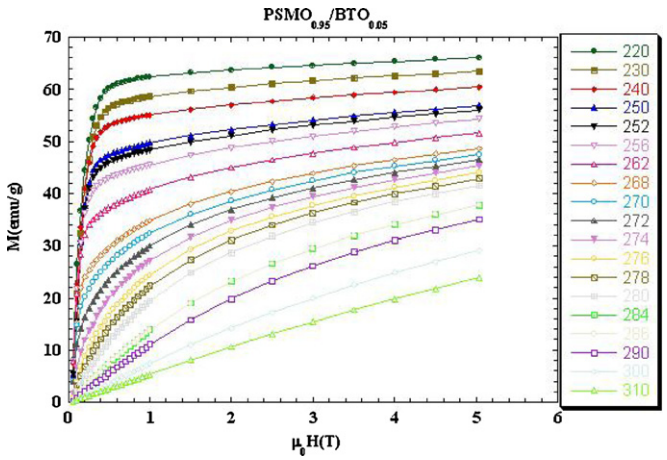

Fig. 4. Isothermal magnetization for $PSMO_{0.95}/BTO_{0.05}$ composite at different temperatures.

sits only at the grain boundaries and on the surfaces of PSMO grains. The same results were found by Keshri et al. [14] in LCMO-BTO composites and also by Kim et al. [19] in LCMO-BTO nanocomposites. However a different result was found by Bose et al. [13] when they obtained a decrease in T_c with the increase of BTO content in the LCMO-BTO composites. These differences could be explained by the difference of the samples preparation methods.

We note also that for $x \leq 0.1$ we did not see any significant change in the value of magnetization at low temperature with the increase of BTO content. This evolution can be attributed to the magnetic order induced by BTO at the grain boundaries, and also to the variation of the strain in the lattice. This effect was observed by Murugavel et al. [17,18] when they investigate the role of ferroelectric–ferromagnetic layers on the properties of superlattice-based multiferroics in PCMO/BST composites.

For $x = 0.3$, the decrease of the magnetization value at low temperature compared to the other samples is attributed to the dilution effect of the ferromagnetic PSMO phase by the ferroelectric BTO phase.

The isothermal magnetization curves for the bulk PB5 compound around its T_c in external magnetic field up to 5 T are shown in Fig. 4. The same behaviour was shown for all other samples with magnetic transition from paramagnetic to ferromagnetic state at the same T_c (≈273 K) as the parent PSMO compound.

3.3. Magnetocaloric properties

The magnetic entropy, which is associated with the magnetocaloric effect, can be calculated from the isothermal magnetization curves versus magnetic applied field. According to the classical thermodynamical theory, the magnetic entropy is related to the magnetization M, the magnetic field H and the absolute temperature T through the Maxwell relation [20,21]:

$$\left(\frac{\partial S(T,H)}{\partial H}\right)_T = \left(\frac{\partial M(T,H)}{\partial T}\right)_H \quad (1)$$

For practical reasons and in order to avoid the difficulties with the adiabatic measurements, the magnetic entropy change ΔS_M was deduced from magnetization isotherms measured in varying magnetic field. The magnetic entropy change ΔS_M produced by the variation of a magnetic field from 0 to H_{max} is given by the following equation:

$$\Delta S_M(T,H) = S_M(T,H) - S_M(T,0) = \int_0^{\mu_0 H_{max}} \left(\frac{\partial M}{\partial T}\right)_H \mu_0\, dH \quad (2)$$

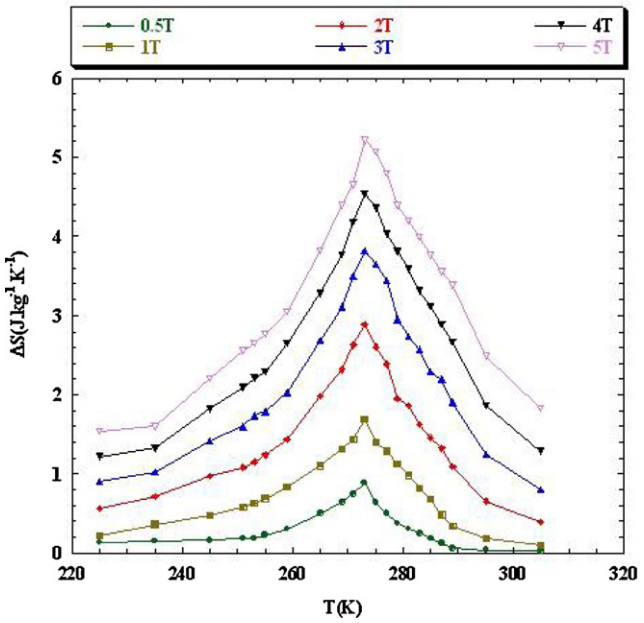

Fig. 5. Magnetic entropy change around the Curie temperature for 0.95PSMO/0.05BTO composite at various magnetic fields.

where $\mu_0 H_{max}$ is the final applied magnetic field.

The equation (Eq. (2)) can be written by:

$$\Delta S_M\left(\frac{T_1+T_2}{2}\right) = \frac{1}{T_2-T_1}\left[\int_0^{\mu_0 H_{max}} M(T_2,\mu_0 H)\mu_0\, dH - \int_0^{\mu_0 H_{max}} M(T_1,\mu_0 H)\mu_0\, dH\right] \quad (3)$$

Hence, $\Delta S_M(T,H)$ can be numerically calculated using (Eq. (3)) and the isothermal magnetization curves versus magnetic applied field for all the samples. The temperature dependence of magnetic entropy change $|\Delta S_M|$ are plotted in Fig. 5 for PB5 sample as an example at various magnetic fields and in Fig. 6 for all samples at an applied magnetic field of 2 T. As seen it is obvious that there is a peak

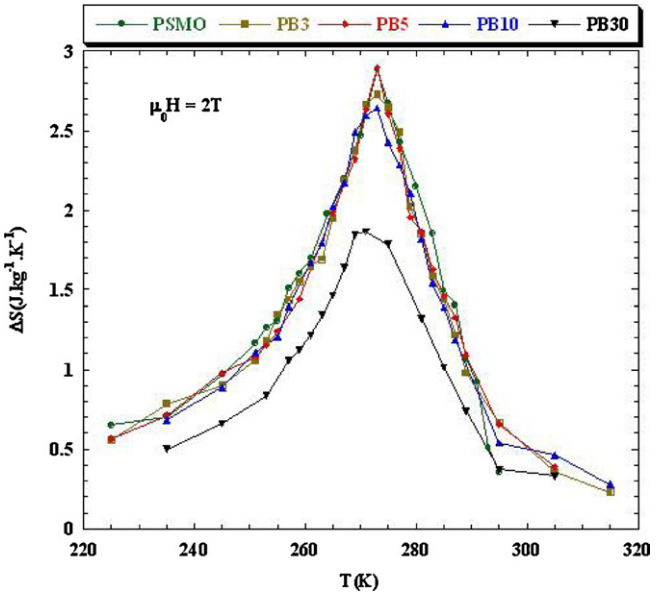

Fig. 6. Magnetic entropy change around the Curie temperature for PSMO/BTO composites at an applied magnetic field of 2 T.

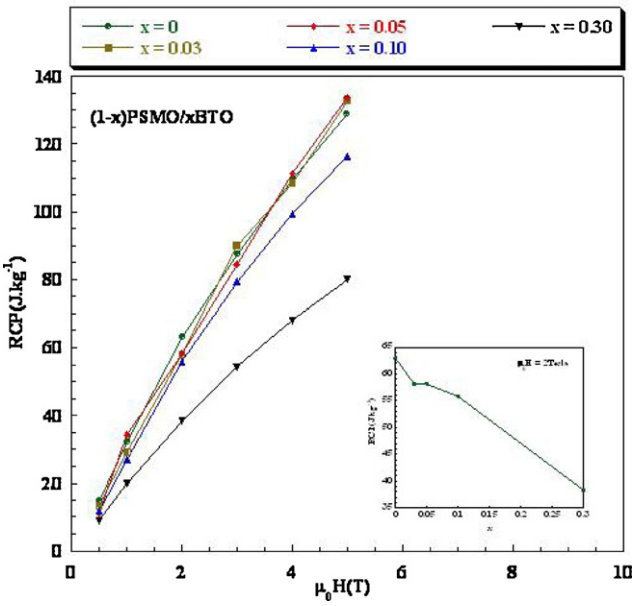

Fig. 7. Relative Cooling Power values (RCP) versus magnetic applied field for PSMO/BTO composites. The inset presents the RCP versus x in $(1-x)$PSMO/xBTO.

in $|\Delta S_M|$ which is defined by $|\Delta S_M^{max}|$ and occurs near the FM–PM transition temperature T_c. $|\Delta S_M^{max}|$ increases with field increasing for each sample, which is indicative of much larger entropy change to be expected at higher magnetic field. The maximum value of the magnetic entropy $|\Delta S_M^{max}|$ does not change and remains almost the same for $x \leq 0.1$, it was found equal to 2.88 J kg^{-1} K^{-1} for $x = 0$ and then decreases to 1.86 J kg^{-1} K^{-1} for $x = 0.3$ for an applied magnetic field of 2 T.

It should be noted that $|\Delta S_M^{max}|$ is not the only parameter deciding about an applicability of material. There is a demand for materials which can transport heat at relatively large temperature difference between the cold and the hot sinks in the ideal refrigeration cycle. This feature is accounted by the full width at half maximum δT_{FWHM} of the $\Delta S_M(T)$ curve. Then the amount of transferred heat may be estimated for an ideal refrigeration cycle by the so called relative cooling power (RCP) defined by [22–24]: $RCP = |\Delta S_M^{max}| \times \delta T_{FWHM}$. RCP values increase with increasing field for all samples and decrease with the increase of BTO content as shown in Fig. 7 and inset. The $|\Delta S_M^{max}|$, δT_{FWHM} and RCP values for all samples at an applied field of 2 T are listed in Table 1. As we can see $|\Delta S_M^{max}|$ and RCP values decrease slightly for the low content of BTO and then strongly for $x > 0.1$ but δT_{FWHM} remains almost unchanged (≈20 K) around T_c.

In order to improve these results theoretically we can estimate the magnetic entropy ΔS_M according to the Landau theory of phase transition and also deduce the order of the magnetic transition. The Landau expansion of the magnetic free energy with the total

Table 1
Values of $|\Delta S_M^{max}|$, δT_{FWHM} and RCP for all samples under an applied field of 2 T.

x	$\lvert\Delta S_M^{max}\rvert$	δT_{FWHM}	RCP
0.00	2.89	21.80	63.00 (2)
0.03	2.72	21.36	58.09 (9)
0.05	2.89	20.13	58.17 (6)
0.10	2.64	21.14	55.81 (0)
0.30	1.86	20.60	38.31 (6)

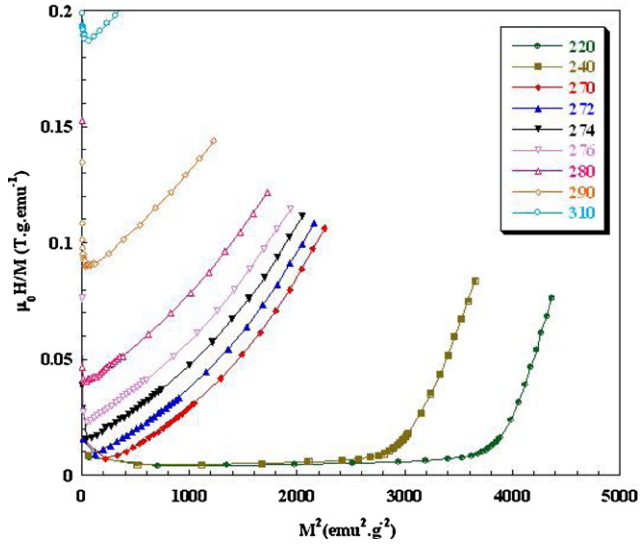

Fig. 8. Arrott plot in the vicinity of T_c for 0.95PSMO/0.05BTO sample at various temperatures.

magnetization, the temperature and the magnetic field is given as [25]:

$$F(M,T) = F_0 + \frac{1}{2}A(T)M^2 + \frac{1}{4}B(T)M^4 + \frac{1}{6}C(T)M^6 - \mu_0 HM \quad (4)$$

The Landau coefficients A, B and C are the thermodynamic parameters depending on temperature, A and C are positive at T_c and B may be positive zero or negative, for $B \geq 0$ at T_c the magnetic transition is of second order and it is first order when $B < 0$ at T_c [26,27].

The Landau theory of ferromagnetism predicts that from the condition of equilibrium in the vicinity of the Curie temperature and by the minimization of the magnetic free energy ($(\partial F(M,T)/\partial M) = 0$), a magnetic equation of state is obtained as:

$$\frac{\mu_0 H}{M} = A + BM^2 + CM^4 \quad (5)$$

The Arrott plots relationship is obtained up to fourth order in the Landau expansion: $(\mu_0 H/M) = A + BM^2$. Fig. 8 shows the Arrott plots near the T_c for the bulk PB5 compound. All the samples of the present series have the same behaviour and they clearly display a positive slope, which indicates a second order phase transition ($B > 0$) [28].

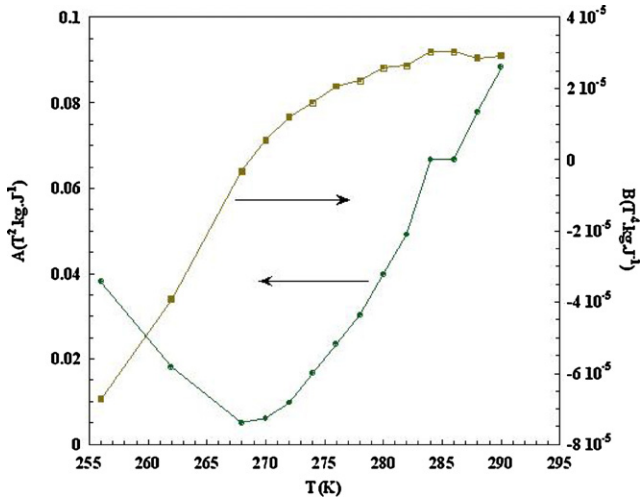

Fig. 9. Temperature dependence of landau coefficients A and B for the 0.95PSMO/0.05BTO sample.

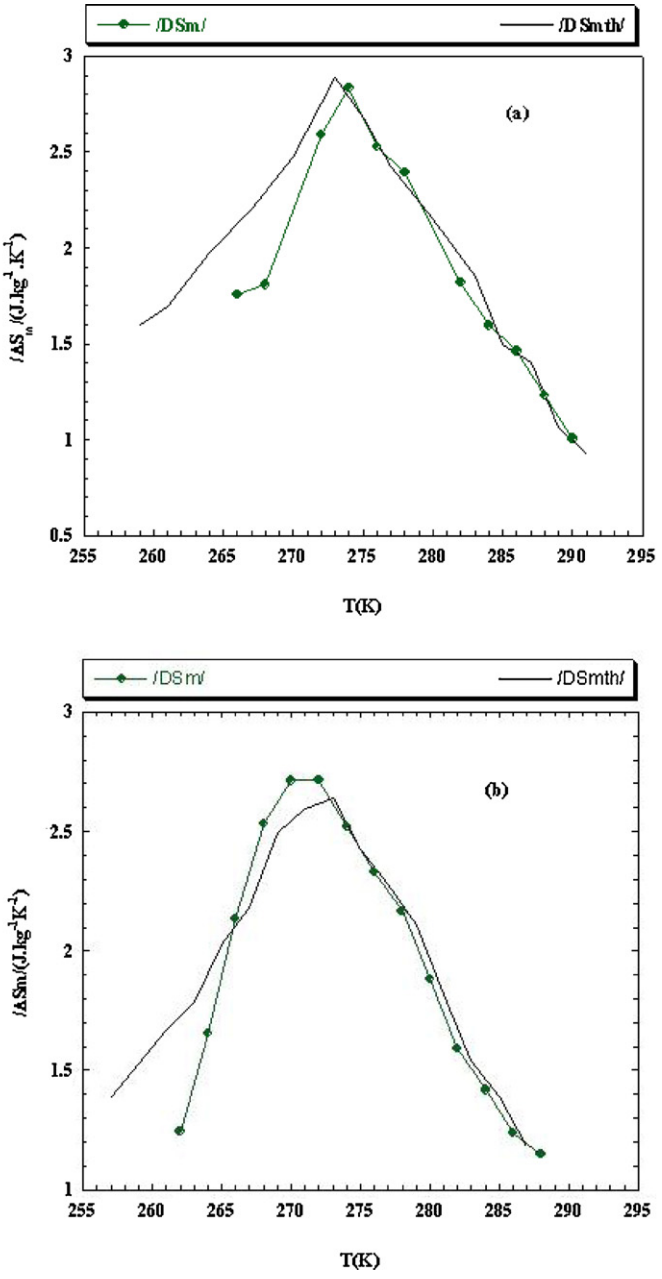

Fig. 10. Experimental and calculated curves of the magnetic entropy change versus temperature upon a magnetic field of 2 T for PSMO (a) and 0.9PSMO/0.1BTO (b) samples.

From Eq. (5) the equation of state linking M and the magnetic field $\mu_0 H$ is:

$$\mu_0 H = AM + BM^3 + CM^5 \quad (6)$$

The temperature dependence of the Landau coefficients $A(T)$, $B(T)$ and $C(T)$ is obtained by fitting the magnetic field $\mu_0 H$ against magnetization using Eq. (6). The results of these fitting are shown in Fig. 9 for the bulk PB5 compound. As expected A is positive with a minimum near T_c and the value of B is positive at T_c confirming the second order magnetic transition at T_c.

The magnetic entropy is obtained from differentiation of the magnetic part of the free energy with respect to temperature:

$$S_M(T,H) = -\left(\frac{\partial F}{\partial T}\right)_H = -\frac{1}{2}A'(T)M^2 - \frac{1}{4}B'(T)M^4 - \frac{1}{6}C'(T)M^6 \quad (7)$$

$A'(T)$, $B'(T)$ and $C'(T)$ are the temperature derivatives of the expansion coefficients. Using Eq. (7), the temperature dependence of the magnetic entropy change $|\Delta S_M|$ is calculated for various applied fields and the results are plotted respectively in Fig. 10a for PSMO and Fig. 10b for PB10 compounds. Circles represent experimental data, while lines show the results obtained by the Landau theory. The model used gives a fairly good description of the temperature dependence of the change in magnetic entropy. This model can be corrected by taking into account the influence of the Jahn–Teller distortion and exchange interaction on the magnetic properties of the manganites.

4. Conclusions

We have studied the magnetocaloric effect on magnetoelectric composites with the general formula $(1-x)(Pr_{0.6}Sr_{0.4}MnO_3)/x(BaTiO_3)$ (with $x = 0.0$, 0.03, 0.05, 0.10 and 0.30) prepared by solid–solid reaction. The presence of BTO has no great effect on the physical properties of PSMO compound. The Curie temperature remains unchanged ($T_c \approx 273$ K). The maximum of magnetic entropy $|\Delta S_M^{max}|$ and RCP values are not very affected for the low content of BTO and decrease for $x > 0.1$. The full width at half maximum δT_{FWHM} of the $\Delta S_M(T)$ curves is ≈20 K around T_c for all the samples. Arrott plots and the temperature dependence of Landau expansion coefficients of magnetic free energy near T_c show a typical second order magnetic transition. The model used to calculate the temperature dependence of the change in magnetic entropy shows a good agreement with experiment results.

Acknowledgements

This work, within the frame work of collaboration, is supported by:

- The Tunisian Ministry of Higher Education and Scientific Research,
- The Portuguese Ministry of Science, Technology and Higher Education.

References

[1] R.N. Mahato, K. Sethupathi, V. Sankaranarayanan, R. Nirmala, J. Magn. Magn. Mater. 322 (2010) 2537.
[2] D.H. Manh, P.T. Phong, T.D. Thanh, L.V. Hong, N.X. Phuc, J. Alloys Compd. 499 (2010) 131.
[3] C.N.R. Rao, B. Raveau (Eds.), Colossal Magnétorésistance, Charge Ordering and Related Properties of Manganese Oxides, World Scientific, Singapore, 1998.
[4] V.P.S. Awana, R. Tripathi, N. Kumar, H. Kishan, G.L. Bhalla, R. Zeng, L.S. Sharth Chandra, V. Ganesan, H.U. Habermeier, J. Appl. Phys. 107 (2010) 09D723.
[5] H. Yang, Z.E. Cao, X. Shen, T. Xian, W.J. Feng, J.L. Jiang, Y.C. Feng, Z.Q. Wei, J.F. Dai, J. Appl. Phys. 106 (2009) 104317.
[6] P.T. Phong, N.V. Khiem, N.V. Dai, D.H. Manh, L.V. Hong, N.X. Phuc, Mater. Lett. 63 (2009) 353.
[7] S.P. Liu, G.D. Tang, Z.Z. Li, W.H. Qi, D.H. Ji, Y.F. Li, W. Chen, D.L. Hou, J. Alloys Compd. 509 (2011) 2320.
[8] K. Gupta, P.C. Jana, A.K. Meikap, T.K. Nath, J. Appl. Phys. 107 (2010) 073704.
[9] L. Joshi, S.S. Rajput, S. Keshri, Phase Transit. 83 (2010) 482.
[10] C. Zener, Phys. Rev. 82 (1951) 403.
[11] H.Y. Hwang, S.W. Cheong, N.P. Ong, B. Balogg, Phys. Rev. Lett. 77 (1996) 2041.
[12] G.M. Ren, S.L. Yuan, H.G. Guan, X. Xiao, G.Q. Yu, J.H. Miao, Y.Q. Wang, S.Y. Yin, Mater. Lett. 61 (2007) 767.
[13] E. Bose, S. Tarana, S. Karmakara, B.K. Chaudhuri, S. Pal, C.P. Sun, H.D. Yang, J. Magn. Magn. Mater. 314 (2007) 30.
[14] S. Keshri (Shaw), L. Joshi, S.K. Rout, J. Alloys Compd. 485 (2009) 501.
[15] B.T. Cong, N.N. Dinh, D.V. Hien, N.L. Tuyen, Physica B 327 (2003) 370.
[16] Z.Y. Zhou, G.S. Luo, F.Y. Jiang, J. Magn. Magn. Mater. 321 (2009) 1919.
[17] P. Murugavel, D. Saurel, W. Prellier, Ch. Simon, B. Raveau, J. Appl. Phys. Lett. 85 (2004) 19.
[18] P. Murugavel, M.P. Singh, W. Prellier, B. Mercey, Ch. Simon, B. Raveau, J. Appl. Phys. 97 (2005) 103914.
[19] Y.N. Kim, E.O. Chi, J.C. Kim, E.K. Lee, N.H. Hur, Solid State Commun. 128 (2003) 339.

[20] A.H. Morrish, The Physical Principles of Magnetism, Wiley, New York, 1965 (Chapter 3).
[21] J.S. Amaral, M.S. Reis, V.S. Amaral, T.M. Mendonc, J.P. Araùjo, M.A. Sà, P.B. Tavares, J.M. Vieira, J. Magn. Magn. Mater. 290–291 (2005) 686–689.
[22] M.H. Phan, S.-C. Yu, J. Magn. Magn. Mater. 308 (2007) 325.
[23] E. Bruck, O. Tegus, X.W. Li, F.R. de Boer, K.H.J. Buschow, Physica B 327 (2003) 431.
[24] M. Pekała, V. Drozd, J. Non-Cryst. Solids 354 (2008) 5308–5314.
[25] J.L. Alonso, et al., Phys. Rev. B 63 (2001) 054411.
[26] V.S. Amaral, J.S. Amaral, J. Magn. Magn. Mater. 272–276 (2004) 2104–2105.
[27] M. Yue, Z.Q. Li, X.B. Liu, H. Xu, D.M. Liu, J.X. Zhang, J. Alloys Compd. 493 (2009) 22.
[28] B.K. Banerjee, Phys. Lett. 12 (1964) 16.